Transgenic Tobacco Plants Overexpressing Chloroplastic Ferredoxin-NADP(H) Reductase Display Normal Rates of Photosynthesis and Increased Tolerance to Oxidative Stress[1]

Ramiro E. Rodriguez, Anabella Lodeyro, Hugo O. Poli, Matias Zurbriggen, Martin Peisker, Javier F. Palatnik, Vanesa B. Tognetti[2], Henning Tschiersch, Mohammad-Reza Hajirezaei, Estela M. Valle, and Néstor Carrillo*

Instituto de Biología Molecular y Celular de Rosario, División Biología Molecular, Facultad de Ciencias Bioquímicas y Farmacéuticas, Universidad Nacional de Rosario, S2002LRK Rosario, Argentina (R.E.R., A.L., H.O.P., M.Z., J.F.P., V.B.T., E.M.V., N.C.); and Leibniz-Institut für Pflanzengenetik und Kulturpflanzenforschung, 06466 Gatersleben, Germany (M.P., H.T., M.-R.H.)

Ferredoxin-NADP(H) reductase (FNR) catalyzes the last step of photosynthetic electron transport in chloroplasts, driving electrons from reduced ferredoxin to $NADP^+$. This reaction is rate limiting for photosynthesis under a wide range of illumination conditions, as revealed by analysis of plants transformed with an antisense version of the FNR gene. To investigate whether accumulation of this flavoprotein over wild-type levels could improve photosynthetic efficiency and growth, we generated transgenic tobacco (*Nicotiana tabacum*) plants expressing a pea (*Pisum sativum*) FNR targeted to chloroplasts. The alien product distributed between the thylakoid membranes and the chloroplast stroma. Transformants grown at 150 or 700 μmol quanta m^{-2} s^{-1} displayed wild-type phenotypes regardless of FNR content. Thylakoids isolated from plants with a 5-fold FNR increase over the wild type displayed only moderate stimulation (approximately 20%) in the rates of electron transport from water to $NADP^+$. In contrast, when donors of photosystem I were used to drive $NADP^+$ photoreduction, the activity was 3- to 4-fold higher than the wild-type controls. Plants expressing various levels of FNR (from 1- to 3.6-fold over the wild type) failed to show significant differences in CO_2 assimilation rates when assayed over a range of light intensities and CO_2 concentrations. Transgenic lines exhibited enhanced tolerance to photooxidative damage and redox-cycling herbicides that propagate reactive oxygen species. The results suggest that photosynthetic electron transport has several rate-limiting steps, with FNR catalyzing just one of them.

Plant photosynthesis takes place in chloroplast-containing source tissues (mostly leaves) that subsequently export the synthesized carbohydrates to heterotrophic sink organs, such as roots or seeds, which depend strictly on the uptake of reduced carbon. The efficiency of this metabolic pathway is thought to be critical for plant growth and crop yield and is therefore a most attractive target for breeders and geneticists (Miyagawa et al., 2001). Accordingly, considerable effort has been devoted to the identification of limiting steps amenable to genetic improvement in both the photosynthetic electron transport chain (PETC) and the reductive pentose phosphate cycle (RPPC). These investigations gained momentum in recent years through the widespread use of antisense RNA technology to reduce the levels of individual proteins and enzymes.

Several components of the RPPC (and other enzymes of carbohydrate metabolism) are known to accumulate in excess, with their in vivo activities modulated through allosteric or covalent (i.e. thiol oxidation) modifications (Buchanan et al., 2002), or indirectly by the supply of inorganic phosphate (Walker and Sivak, 1986). As a consequence, decreases in protein levels caused by the introduction of antisense RNA in transgenic plants are partially compensated by further activation of the extant enzyme molecules, resulting in attenuation of the inhibitory effects. For example, rates of photosynthesis were not strongly affected until the content of Rubisco (Stitt et al., 1991; Hudson et al., 1992), aldolase (Haake et al., 1998), plastidic Fru-1,6-bisphosphatase (Kossmann et al., 1994), sedoheptulose-1,7-bisphosphatase (Harrison et al., 1998), and phosphoribulokinase (Paul et al., 1995) was reduced to 50% or less of their wild-type levels. Moreover, the effects usually became significant only under saturating CO_2 and illumination (Stitt et al., 1991). In spite of this grim prognosis, Miyagawa et al. (2001) obtained enhanced photosynthetic efficiency, growth

[1] This work was supported by the National Agency for the Promotion of Science and Technology (PICT'99 grant no. 01–5105 and PICT'03 grant no. 01–14684) and Fundación Antorchas, Argentina.

[2] Present address: Department of Plant Physiology and Biochemistry/W5, University of Bielefeld, 33501 Bielefeld, Germany.

* Corresponding author; e-mail carrillo@ibr.gov.ar; fax 54–341–4390465.

The author responsible for distribution of materials integral to the findings presented in this article in accordance with the policy described in the Instructions for Authors (www.plantphysiol.org) is: Néstor Carrillo (carrillo@ibr.gov.ar).

www.plantphysiol.org/cgi/doi/10.1104/pp.106.090449

rates, and biomass accumulation by targeting a cyanobacterial Fru-1,6-/sedoheptulose-1,7-bisphosphatase to chloroplasts of transgenic tobacco (*Nicotiana tabacum*). In contrast, attempts to manipulate the allocation of carbon assimilates by expressing ADP-Glc pyrophosphorylase from *Escherichia coli* in amyloplasts of potato (*Solanum tuberosum*) tubers (Stark et al., 1992) or a maize (*Zea mays*) Suc phosphate synthase in the cytosol of tomato (*Lycopersicon esculentum*) leaf cells (Galtier et al., 1993) met with only moderate success.

On the other hand, relatively few investigations have been carried out with genotypes differing in PETC components. Transgenic plants in which the content of ferredoxin (Fd; Holtgrefe et al., 2003) or the Rieske iron-sulfur (FeS) protein of the cytochrome b_6f complex (Price et al., 1998) were diminished by expression of antisense RNA exhibited lower CO_2 assimilation rates, which correlated fairly well with the levels of remaining protein. Using a similar strategy, we restrained the expression of chloroplast Fd-NADP(H) reductase (FNR), a flavin adenine dinucleotide-containing enzyme that catalyzes the final step of the PETC, namely, electron transfer from reduced Fd to $NADP^+$ (Hajirezaei et al., 2002). Plants containing 20% to 70% of the reductase present in nontransformed siblings displayed growth arrest, chlorophyll (chl) degradation, and impaired CO_2 uptake. They were also abnormally prone to photooxidative damage (Palatnik et al., 2003). Control analysis revealed that FNR mediates a rate-limiting step of photosynthesis under both limiting and saturating light conditions (Hajirezaei et al., 2002), raising the possibility that overexpression of this flavoprotein could stimulate photosynthesis and ultimately lead to increased biomass production.

To probe this contention, we constructed transgenic tobacco plants expressing a pea (*Pisum sativum*) FNR in chloroplasts. The foreign flavoprotein accumulated up to 6-fold over the levels of its indigenous counterpart. Contrary to our expectations, however, transformants grown at low or high irradiation exhibited phenotypes and photosynthetic activities comparable to those of their wild-type siblings. Rates of $NADP^+$ photoreduction by isolated thylakoids correlated with FNR content only when electron donors of PSI were employed to drive the reaction. CO_2 assimilation rates did not differ significantly between wild type and transformants with an approximately 4-fold increase in FNR levels. Interestingly enough, lines overexpressing the reductase showed augmented tolerance to photooxidative damage and redox-cycling oxidants.

RESULTS

Generation of Transgenic Tobacco Plants Expressing Pea FNR in Chloroplasts

To obtain plants with increased levels of FNR activity in chloroplasts, we cloned a full-length cDNA encoding the pea FNR precursor (Newman and Gray, 1988) between the constitutive cauliflower mosaic virus (CaMV) 35S promoter and terminator sequences in the binary vector pCAMBIA2200 (Fig. 1A) and introduced the construct in tobacco (cv Petit Havana) via *Agrobacterium tumefaciens* transformation (see "Materials and Methods"). Several plants originating from independent transformation events were regenerated in selective medium and tested for FNR expression by RNA analysis (data not shown) and immunoblotting of total leaf extracts (Fig. 1B). Mature regions of pea and tobacco reductases contain 308 residues and display 88% of sequence identity at the amino acid level (Newman and Gray, 1988; Hajirezaei

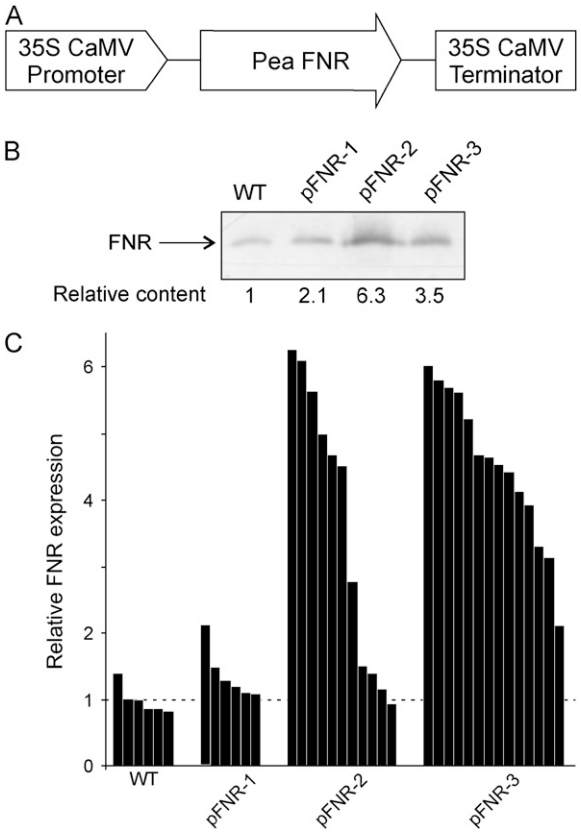

Figure 1. Overexpression of Fd-NADP(H) reductase in transgenic tobacco plants. A, Schematic representation of the chimeric gene used to generate transgenic plants overexpressing FNR. The coding sequence of pea FNR was cloned between the CaMV 35S promoter and polyadenylation regions. B, FNR accumulation in leaves of wild type and three independent primary transformants. Leaf extracts from 6-week-old plants corresponding to 5 μg protein were fractionated by SDS-PAGE and blotted onto nitrocellulose membranes for immunodetection of FNR with antisera directed against the pea reductase. Arrow shows the electrophoretic mobility of FNR. Numerals below each lane indicate the FNR content relative to that of the wild-type line, as determined by densitometric scanning of the immunoblots. C, Comparative amounts of FNR in wild-type and transgenic tobacco plants. Primary transformants were propagated up to the T_2 generation by self pollination and the accumulation of FNR was determined by quantitative scanning of immunoblots as those in B and normalized with respect to the average FNR levels found in wild-type plants. Each bar corresponds to an individual specimen from the indicated line.

et al., 2002). Not unexpectedly, therefore, the corresponding proteins exhibited similar electrophoretic mobility when resolved by SDS-PAGE and cross-reacted with an antiserum raised against pea FNR (Fig. 1B). Lanes 2 to 4 in Figure 1B illustrate typical examples of primary transformants (T_0 generation) containing significantly higher levels of immunoreactive protein (2.1- to 6.3-fold) over nontransformed siblings. Primary transformants were propagated up to the T_2 generation by self pollination and accumulation of FNR was determined by western-blot analysis. In most cases, progeny were not uniform and varied in the amount of FNR accumulated, suggesting that multiple transgene copies inserted at different loci were segregating. This behavior has frequently been observed using other transgenic plants (Stitt et al., 1991; Harrison et al., 1998; Hajirezaei et al., 2002). Representative segregation patterns of three independent lines displaying low (pFNR-1), high (pFNR-3), or variable (pFNR-2) reductase levels are shown in Figure 1C. In view of this unpredictable behavior, the actual FNR amount was measured in the respective leaf for any biochemical or physiological experiment and is specified in the legends to figures and tables.

Although FNR is highly specific for NADP(H) and a very poor NAD(H)-dependent oxidoreductase, it can derive electrons to a wide variety of acceptors of appropriate redox potential but very different structures, mediating the so-called diaphorase reaction (Carrillo and Ceccarelli, 2003). Expression of pea FNR in tobacco chloroplasts led to a concomitant increase in diaphorase activity (Fig. 2, A and B), indicating that the introduced flavoenzyme was functional in the transgenic host. It could be recognized as an extra band of lower electrophoretic mobility when soluble extracts from transgenic plants were separated by native PAGE and stained for diaphorase activity (Fig. 2B).

Leaf homogenates of the various transformants contained no trace of FNR precursor (Fig. 1B), suggesting that the pea-derived flavoprotein was correctly imported and processed by tobacco plastids. To corroborate this subcellular location, we prepared lysates from whole leaves and isolated chloroplasts and subjected them to SDS-PAGE and immunoblotting. When identical amounts of chl were loaded, nearly all FNR was recovered in the chloroplastic fraction of both wild-type and transgenic plants (Fig. 2C), indicating that the foreign enzyme was indeed plastid targeted.

Plant FNR is regarded as a thylakoid-bound protein (Vallejos et al., 1984). Accordingly, when chloroplasts isolated from nontransformed plants were ruptured by osmotic shock, most of the reductase was recovered in the membrane fraction (Fig. 2D, lanes 1 and 3). The extent of FNR solubilization increased by harsher extraction procedures, such as grinding of the leaves (Fig. 2B) or chloroplasts (data not shown) at the temperature of liquid nitrogen, confirming that it is not an integral protein (Vallejos et al., 1984). Part of the pea-derived enzyme also attached to the host thylakoids and was not removed by exhaustive washing, but a significant proportion remained soluble in the stroma (Fig. 2, A and D [lanes 2 and 4]). Interaction of FNR with the membrane is mediated by intrinsic proteins (Vallejos et al., 1984; Andersen et al., 1992; Zhang et al., 2001) and these binding sites might be titrated as enzyme levels build up in transgenic plants.

Effects of FNR Overexpression on Plant Growth and Photosynthesis

Transformants of the T_2 generation were used for phenotypic analysis. They grew as their nontransformed siblings when cultivated in a growth chamber at moderate light intensities (150 μmol quanta $m^{-2}\,s^{-1}$) and contained similar amounts of leaf chl and carotenoids per unit leaf area (Table I). Maximal CO_2 assimilation rates at saturating light intensity and ambient CO_2 concentrations were 19 to 20 μmol CO_2 $cm^{-2}\,s^{-1}$ for all lines and were even slightly lower (approximately 15% relative to the wild type) in plants overexpressing FNR when assayed at saturating CO_2 and two different light intensities (Table I). Photosynthetic parameters reflecting photon capture and integrity of PSII (F_v/F_m), electron transport (ϕ_{PSII}), and nonphotochemical quenching (NPQ) were also similar in all lines regardless of FNR content (Table I).

To rule out the possibility that the lack of increase in photosynthesis and biomass accumulation was caused by remodeling of the photosynthetic apparatus during growth under relatively low light intensities, plants were also cultured at 700 μmol quanta $m^{-2}\,s^{-1}$ with the same photoperiod and a daytime temperature of 29°C. Once again, the various transgenic and wild-type plants failed to show significant differences in fresh or dry weight, chl and carotenoid content, CO_2 assimilation rates, or the F_v/F_m, ϕ_{PSII}, and NPQ values (Table I).

Plants from all lines were, on average, 35% shorter and contained approximately 50% less chl per unit leaf area when compared to siblings grown at 150 μmol quanta $m^{-2}\,s^{-1}$ (Table I). This behavior has been regularly observed in plants cultured under similar conditions (Flachmann, 1997; Pierik et al., 2004), presumably reflecting the need to optimize photon capture from limited light sources. Growth at 700 μmol quanta $m^{-2}\,s^{-1}$ resulted in considerable decreases in fresh weight (approximately 35% on average) and dry weight (approximately 19% on average), although the fraction of biomass, calculated as the dry weight-to-fresh weight ratio, was significantly higher in plants grown under these conditions (approximately 9.2% on average), with respect to siblings cultured at lower light intensities that accumulated, on average, 7.2% of dry matter (Table I). Maximal CO_2 fixation rates were slightly higher (approximately 25% on average) when the plants cultured in the higher light regime were assayed at saturating CO_2, but not when evaluated at saturating light intensity and ambient CO_2 concentrations (Table I). Reasons for the decrease in absolute biomass in highly irradiated specimens are unclear. Lack of photooxidative damage revealed by similar

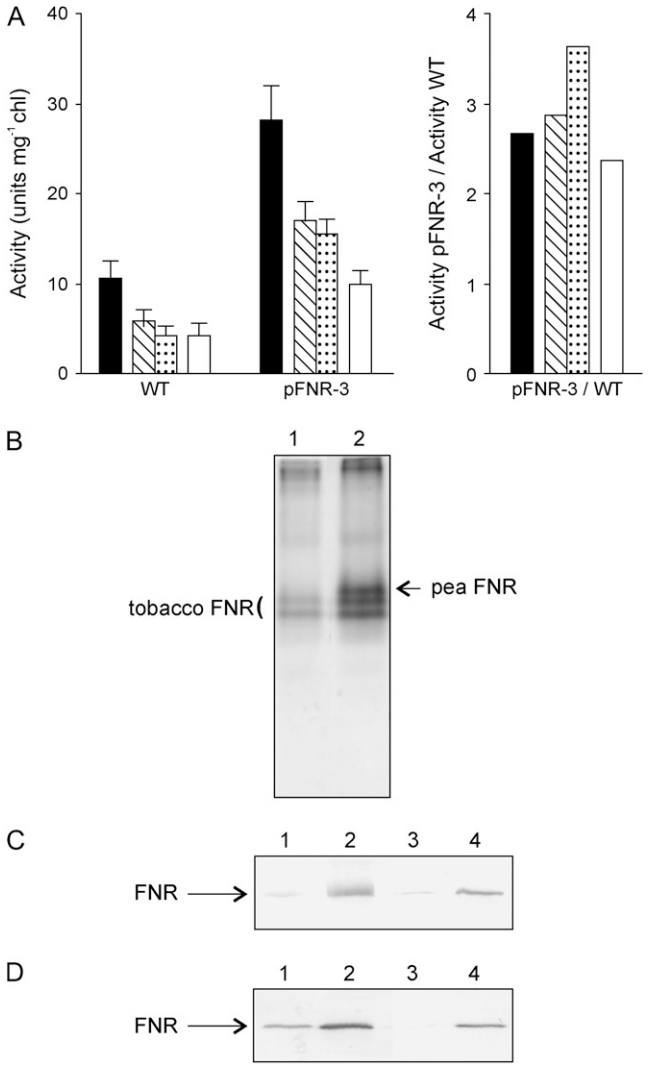

Figure 2. Activity and subcellular localization of FNR in transgenic plants. A, FNR activity in thylakoids and stromal extracts of wild-type and FNR-expressing plants. Intact chloroplasts were isolated from 6-week-old wild-type and pFNR-3 plants and osmotically shocked. Stroma was separated by centrifugation and the resulting thylakoid pellet washed four times in hypotonic medium. NADPH-ferricyanide diaphorase activity was measured in whole broken chloroplasts (black bars), thylakoids washed two (hatched bars) or four (dotted bars) times, and stroma (white bars). The activity ratio represents the increase of diaphorase activity in each fraction of pFNR-3 relative to wild-type chloroplasts. B, Electrophoretic mobility of pea-derived FNR during nondenaturing PAGE of tobacco leaf extracts. Cleared lysates from wild-type (lane 1) and pFNR-3 leaves (lane 2), corresponding to 20 μg of total soluble protein, were resolved by native electrophoresis and stained for diaphorase activity. Tobacco and pea FNR isoforms are indicated. C, Subcellular localization of FNR in pFNR-3 plants. Total leaf extracts (lanes 1 and 2) and isolated chloroplasts (lanes 3 and 4) from 6-week-old wild-type (lanes 1 and 3) or pFNR-3 (lanes 2 and 4) plants were fractionated by SDS-PAGE and blotted onto nitrocellulose membranes for immunodetection of FNR. Samples corresponding to 5 μg chl were loaded onto each lane. D, Suborganellar localization of FNR. Thylakoids (lanes 1 and 2) and stroma (lanes 3 and 4) were separated after osmotic shock of isolated intact chloroplasts from wild-type (lanes 1 and 3) and pFNR-3 (lanes 2 and 4) plants. Samples corresponding to 5 μg chl were resolved by SDS-PAGE and the presence of FNR was determined by immunoblot analysis.

F_v/F_m and NPQ values (Table I) indicates that these plants were not stressed from excess light or water deficit. The different conditions at which the plants were grown precluded a more detailed analysis of the causes. In spite of the growth rate variations observed between the two culture conditions, it is clear from the observations summarized in Table I that FNR overexpression did not improve photosynthetic rates and biomass deployment under any of them. The collected results suggest that steps other than $NADP^+$ photoreduction could be limiting photosynthesis.

To evaluate this possibility, we measured photosynthetic electron transport by thylakoids isolated from wild-type and pFNR-3 plants that contained FNR, on average, 4.6-fold over wild-type levels. Water-driven $NADP^+$ photoreduction rates were 0.57 $\pm$ 0.11 and 0.67 $\pm$ 0.12 μmol NADPH mg^{-1} chl min^{-1} ($P < 0.05$) for wild-type and pFNR-3 plastids, respectively, corresponding to an increase of only 20% (Fig. 3A). When the ascorbate/*N*,*N*,*N*′,*N*′-tetramethyl-*p*-phenylendiamine (TMPD) pair was employed as a PSI electron donor in the presence of 3-(3,4-dichlorophenyl)-1,1-dimethyl urea (DCMU), an inhibitor that prevents electron transfer from PSII, pFNR-3 chloroplasts displayed approximately 3-fold more activity (2.36 $\pm$ 0.31 μmol NADPH mg^{-1} chl min^{-1}) than wild-type plastids (0.74 $\pm$ 0.15 μmol NADPH mg^{-1} chl min^{-1}; Fig. 3B). In contrast, light-driven reduction of methyl viologen (MV) proceeded at similar rates in all lines, with specific activity of 2.05 $\pm$ 0.25 and 1.93 $\pm$ 0.31 μmol O_2 mg^{-1} chl min^{-1} for wild type and pFNR-3 thylakoids, respectively.

Plants Accumulating FNR Display Increased Tolerance to Photooxidative Damage and Redox-Cycling Herbicides

FNR-deficient plants were highly sensitive to photoinactivation, undergoing leaf bleaching, lipid peroxidation, and membrane damage even under moderate irradiation (Palatnik et al., 2003). The magnitude of the effect was directly dependent on the light intensity and the extent of FNR depletion. We therefore decided to evaluate the performance of plants overexpressing the enzyme when faced with this environmental hardship. Figure 4 shows that leaf discs from transformants accumulating FNR over wild-type levels displayed increased tolerance to high irradiation, reflected by preservation of chl content (Fig. 4A) and membrane integrity (Fig. 4B).

After photooxidative treatment resulting from a combination of relatively high light intensity (700 μmol quanta m^{-2} s^{-1}) and low temperature (8°C), the maximal quantum efficiency of PSII photochemistry (F_v/F_m) was reduced to a lower value in wild-type plants in comparison to plants overexpressing FNR (Fig. 4C). Decreases in F_v/F_m can be due to photodamage to PSII reaction centers as well as to the development of

Table I. *FNR overexpression in chloroplasts does not affect growth and photosynthetic parameters in transgenic tobacco plants*

Tobacco plants from the indicated transgenic lines were germinated in soil and grown for 6 weeks in a growth chamber at two light intensities. Relative FNR amounts were calculated by western-blot analysis. Results are means ± SE of four individuals for wild-type and pFNR-1 plants and eight individuals for pFNR-3 plants. Aerial fresh and dry weights were measured in vegetative tissues, including leaves and stem. nd, Not determined.

	Growth Condition					
	150 μmol quanta m^{-2} s^{-1}			700 μmol quanta m^{-2} s^{-1}		
	Wild Type	pFNR-1	pFNR-3	Wild Type	pFNR-1	pFNR-3
Relative FNR amount	1.0 ± 0.2	1.1 ± 0.2	3.4 ± 0.8	1.0 ± 0.1	1.0 ± 0.4	3.6 ± 0.9
Height (cm)	57.0 ± 3.0	51.7 ± 7.1	45.5 ± 3.4	43.7 ± 3.9	37.7 ± 3.4	33.8 ± 1.9
Aerial fresh weight (g)	82.3 ± 8.0	77.5 ± 3.5	77.3 ± 5.0	52.1 ± 3.4	51.9 ± 4.9	49.3 ± 2.1
Aerial dry weight (g)	6.2 ± 0.4	6.0 ± 0.7	5.0 ± 0.4	4.9 ± 0.2	4.7 ± 0.5	4.3 ± 0.4
Dry weight/fresh weight (%)	7.5 ± 0.9	7.7 ± 2.1	6.5 ± 0.9	9.4 ± 1.4	9.4 ± 1.8	8.7 ± 2.4
Chl (μg cm^{-2})	37.5 ± 2.9	33.4 ± 1.6	32.8 ± 3.9	18.4 ± 4.4	17.7 ± 1.9	16.1 ± 4.4
Chl *a*/*b*	2.4 ± 0.1	2.4 ± 0.2	2.4 ± 0.1	2.4 ± 0.2	2.3 ± 0.1	2.5 ± 0.2
Total carotenoids (μg cm^{-2})	6.1 ± 0.4	5.5 ± 0.5	5.6 ± 0.6	4.4 ± 0.5	4.2 ± 0.5	3.8 ± 0.8
F_v/F_m	0.79 ± 0.01	0.80 ± 0.02	0.80 ± 0.01	0.78 ± 0.02	0.77 ± 0.02	0.78 ± 0.02
ϕ_{PSII} at 150 μmol quanta m^{-2} s^{-1}	0.71 ± 0.01	0.70 ± 0.01	0.70 ± 0.02	0.70 ± 0.01	0.70 ± 0.01	0.7 ± 0.01
ϕ_{PSII} at 1,000 μmol quanta m^{-2} s^{-1}	0.32 ± 0.02	0.32 ± 0.06	0.31 ± 0.07	0.42 ± 0.02	0.41 ± 0.04	0.41 ± 0.02
NPQ at 150 μmol quanta m^{-2} s^{-1}	0.23 ± 0.03	0.23 ± 0.02	0.24 ± 0.03	0.22 ± 0.03	0.20 ± 0.04	0.20 ± 0.04
NPQ at 1,000 μmol quanta m^{-2} s^{-1}	1.93 ± 0.14	1.83 ± 0.46	1.84 ± 0.46	1.00 ± 0.19	1.22 ± 0.31	1.06 ± 0.26
1 − qP at 150 μmol quanta m^{-2} s^{-1}	0.07 ± 0.01	0.10 ± 0.01	0.10 ± 0.02	0.07 ± 0.01	0.05 ± 0.02	0.07 ± 0.01
1 − qP at 1,000 μmol quanta m^{-2} s^{-1}	0.34 ± 0.03	0.38 ± 0.04	0.41 ± 0.09	0.27 ± 0.07	0.23 ± 0.05	0.30 ± 0.08
A_{CO2} versus light intensity[a]						
Initial slope	0.074 ± 0.005	0.076 ± 0.011	0.071 ± 0.007	0.058 ± 0.006	0.066 ± 0.004	0.068 ± 0.011
A_{max} (μmol CO_2 cm^{-2} s^{-1})	19.43 ± 3.23	19.86 ± 2.34	19.81 ± 4.22	17.23 ± 4.01	23.79 ± 4.14	19.64 ± 3.11
A_{CO2} versus Ci at 400 μmol quanta m^{-2} s^{-1}[b]						
Initial slope	0.055 ± 0.006	nd	0.055 ± 0.010	0.101 ± 0.050	0.072 ± 0.017	0.064 ± 0.016
A_{max} (μmol CO_2 cm^{-2} s^{-1})	18.25 ± 1.91	nd	15.89 ± 1.56	21.75 ± 1.76	19.30 ± 1.49	20.84 ± 1.44
A_{CO2} versus Ci at 2,000 μmol quanta m^{-2} s^{-1}[b]						
Initial slope	0.075 ± 0.009	nd	0.070 ± 0.006	0.059 ± 0.021	0.085 ± 0.017	0.067 ± 0.030
A_{max} (μmol CO_2 cm^{-2} s^{-1})	31.45 ± 2.31	nd	25.51 ± 4.25	37.63 ± 5.41	35.67 ± 3.36	34.90 ± 3.85

[a]The net CO_2 uptake rate at saturating light (A_{max}) and the initial slope at low light intensity were derived from light response curves by fitting experimental data to the equation of a nonrectangular hyperbola as described (Hajirezaei et al., 2002). [b]The net CO_2 uptake rate at saturating CO_2 internal concentration (A_{max}) and the initial slope at low Ci were derived from Ci response curves by fitting experimental data to the equation of a nonrectangular hyperbola as described (Hajirezaei et al., 2002).

slowly relaxing NPQ (Baker and Rosenqvist, 2004). No differences were observed in the deactivation kinetics of the energy-dependent NPQ values between wild-type and transgenics plants (data not shown). Thus, the higher F_v/F_m values measured after photooxidative treatment of pFNR-3 plants suggest that light-driven damage to PSII was ameliorated in transformants relative to wild-type siblings.

Oxidative damage can also be inflicted by subjecting plants to the toxic effects of MV, an herbicide that propagates superoxide anion radicals through a redox-cycling reaction of the reduced form with molecular oxygen (Babbs et al., 1989). FNR antisense plants were not especially sensitive to this compound, presumably because their chloroplasts had impaired MV photoreduction (Hajirezaei et al., 2002), which is a mandatory step for the manifestation of toxicity (Babbs et al., 1989). As reported in the preceding overexpressing FNR in chloroplasts displayed wild-type rates of MV photoreduction. These lines were more tolerant than wild-type tobacco to MV-dependent leaf bleaching (Fig. 5A), pigment degradation (Fig. 5B), ion leakage (Fig. 5C), and inactivation of photosynthesis, as indicated by the decrease in ϕ_{PSII} (Fig. 5D). Rubisco has been identified as an early and very sensitive target of oxidative stress, undergoing oxidative cleavage and degradation of the large subunit (LSU) both in vivo and in vitro (Desimone et al., 1996; Palatnik et al., 1999). LSU levels declined in both wild-type and FNR-expressing plants after exposure to MV, but degradation was partially prevented in the transformants relative to the wild type (Fig. 5E). The results indicate that FNR accumulation led to stress-tolerant plants that were able to survive and carry on photosynthesis under conditions that were detrimental to their non-transformed siblings.

DISCUSSION

FNR catalyzes a key step of photosynthetic electron transport, collecting one electron from each of two molecules of reduced Fd in its flavin cofactor to convey a hydride group to $NADP^+$ in a single elementary

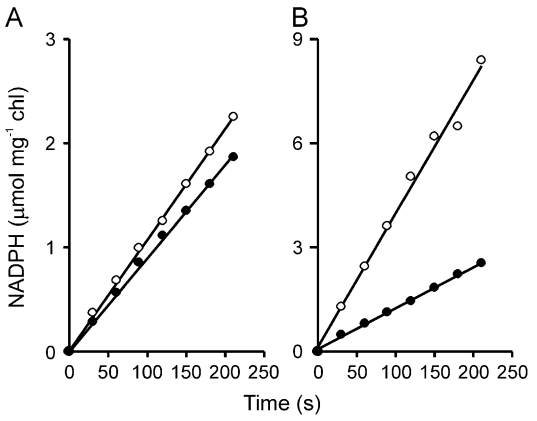

Figure 3. Rates of $NADP^+$ photoreduction by thylakoids from wild-type and transgenic plants overexpressing FNR. $NADP^+$ photoreduction activity by thylakoids isolated from 6-week-old wild-type (black circles) or transgenic plants accumulating 4.6-fold FNR over the wild-type levels (white circles) were measured as indicated in "Materials and Methods," using either water (A) or ascorbate-TMPD (B) as electron donors. DCMU was added to a final concentration of 2.2 μM in the latter case to prevent electron transport from PSII. Reaction rates (in μmol NADPH mg^{-1} chl min^{-1}) were 0.57 (wild type) and 0.67 (pFNR-3) in A and 0.74 (wild type) and 2.36 (pFNR-3) in B.

reaction (Bruns and Karplus, 1995; Carrillo and Ceccarelli, 2003). Whereas many functional properties of FNR have been thoroughly characterized (Carrillo and Ceccarelli, 2003; Ceccarelli et al., 2004), until recently, little was known on the actual contribution of this flavoenzyme to electron transport and photosynthesis in planta. The combined use of FNR antisense (Hajirezaei et al., 2002) and overexpressing transgenic plants (this work) revealed somehow paradoxical behavior. Net CO_2 fixation rose steeply with FNR content in antisense plants until wild-type levels were reached, but further accumulation failed to increase photosynthetic rates over wild-type values (Fig. 6). The lack of effect could be due, in part, to mistargeting of the introduced protein to the chloroplast stroma instead of the thylakoids (Fig. 2D), taking into account that the ability of the soluble form of FNR to engage in photosynthetic electron transport is very limited (Forti and Bracale, 1984; Nakatani and Shin, 1992). However, a considerable fraction of the transgenic product was rescued in a membrane-bound form (Fig. 2D) and was shown to display full activity in the ferricyanide reduction assay (Fig. 2A).

The failure of FNR to boost carbon assimilation when expressed beyond wild-type levels might reflect the existence of tight coordination in the relative proportions and reaction rates at which components of the PETC operate, resulting in more than one rate-limiting step. Depletion of some chain intermediates could lead to impairment of photosynthesis, but, as their levels build up (e.g. in transgenic plants), other components become immediately limiting so that the overall output of the process is hardly changed. Therefore, even when functional FNR molecules were incorporated into the thylakoid membranes in the transformants, $NADP^+$ photoreduction could still be restrained if the provision of reduced Fd is already limited by a previous step. This contention gained support from the observation that thylakoids isolated from plants overexpressing FNR displayed at least 3-fold higher $NADP^+$ photoreduction activity with respect to wild-type membranes when electron transfer from water to $NADP^+$ was blocked at the reducing side of PSII, and PSI electron donors were provided, therefore bypassing electron transfer processes from water to plastocyanin (Fig. 3A). These data suggest that at least an additional rate-limiting step does exist either between photosystems or at the oxidizing side of PSII.

Electron transport in thylakoids involves the function of four membrane-bound components (the PSII/oxygen evolution, cytochrome b_6f and PSI complexes, and FNR) linked by three electron transfer processes mediated by the diffusible components plastoquinone, plastocyanin, and Fd (Haehnel, 1984). Movement of one electron along the PETC proceeds with turnover times of 5 to 10 ms in the steady state (Haehnel, 1984). The search for rate-limiting steps has largely focused on diffusion-limited reactions. The slowest process of linear electron transport with a half time of 15 ms has been ascribed to reactions involved in plastoquinol oxidation, including electron transfer and plastoquinol diffusion in the lipid bilayer from its reduction site in PSII to the cytochrome b_6f complex (Witt, 1971). Plastocyanin-mediated cytochrome *f* oxidation by $P700^+$ occurs within 0.3 ms in spinach (*Spinacia oleracea*) chloroplasts (Haehnel et al., 1980). With respect to the reducing side of PSI, Bouges-Bocquet (1980) has measured the Fd-mediated one- electron reduction of FNR to the neutral semiquinone in a time frame of only 3 μs at 273 K in Chlorella cells. However, steady-state rates are certainly much slower because the rate-limiting step of this process is dissociation of oxidized Fd from its binding site in FNR, a requisite for the entrance of the second Fd molecule that allows the reaction to complete (Batie and Kamin, 1984). Indeed, electron transfer from reduced Fd to FNR in the presence of purified PSI particles and saturating amounts of $NADP^+$ proceeds at approximately 200 s^{-1} (Cassan et al., 2005), corresponding to reaction times of approximately 3 ms. In addition, some of the reactions involved in electron transfer within the cytochrome b_6f complex have been dissected using flash kinetic spectroscopy. Soriano et al. (2002) determined that reduction of cytochrome *f* by the Rieske FeS protein proceeds at 150 to 250 s^{-1}, with tethered movement of the protein from its quinol-proximal site to a region close to the cytochrome *f* heme representing the slowest process that limits the reaction. By comparison, other processes of the PETC take place much faster, with rate constants of approximately 800 s^{-1} for Fd reduction by PSI (Cassan et al., 2005), and 2,400 to 3,000 s^{-1} for electron transfer from cytochrome *f* to plastocyanin (Soriano et al., 2002). The results indicate

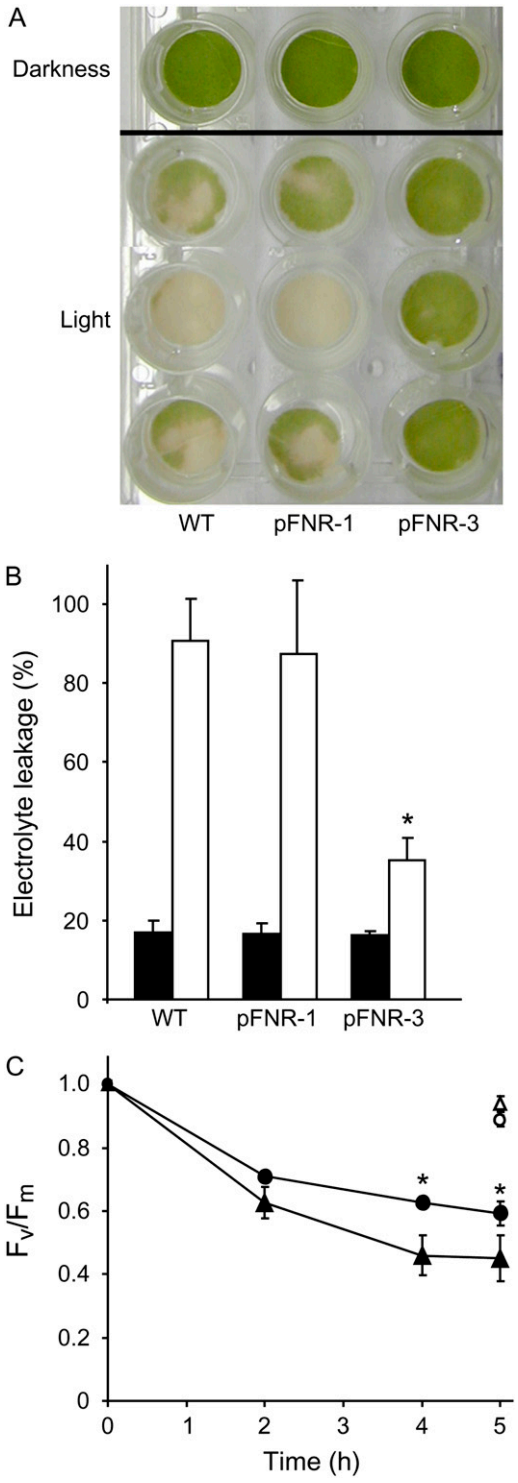

Figure 4. Effect of excess irradiation on wild-type and FNR-expressing plants. Bleaching (A) and membrane damage (B) were analyzed in leaf discs from 6-week-old wild-type and transgenic plants exposed to 2,000 μmol quanta m^{-2} s^{-1} for 17 h at 28°C. The pFNR-1 and pFNR-3 plants employed contained 1.2- and 3.2-fold more reductase than their wild-type siblings. C, Light-dependent damage to PSII as estimated by the decrease in F_v/F_m. Leaf discs from wild-type (triangles) or pFNR-3 (circles) plants were irradiated with 700 μmol quanta m^{-2} s^{-1} at 8°C during the indicated times. White symbols correspond to discs kept in the dark at the same temperature. The transformant employed contained 4.5-fold more reductase than its wild-type sibling. Asterisks indicate significant differences between transgenic and wild-type plants by ANOVA ($P < 0.05$).

that cytochrome *f* and FNR reduction occur within the same time frame and may thus represent as many rate-limiting steps of oxygenic photosynthesis, even though plastoquinol diffusion and/or oxidation could still be slightly slower (Haehnel, 1984).

In agreement with the kinetic determinations, plants expressing an antisense version of the gene encoding the Rieske FeS protein exhibited phenotypes that shared many common features with those of FNR-deficient lines (Price et al., 1998; Hajirezaei et al., 2002). Antisense potato plants with decreased levels of Fd also displayed growth penalties, but attenuated with respect to those caused by depletion of FNR or the Rieske FeS protein (Holtgrefe et al., 2003). The milder phenotype is probably related to the fact that Fd is engaged in electron distribution to other chloroplast processes besides $NADP^+$ reduction and therefore accumulates above the levels of other PETC components, reaching a concentration of about 80 μM (Yonekura-Sakakibara et al., 2000). In line with the observations reported here for plants accumulating higher content of FNR, overexpression of shuttle members of the PETC, such as Fd (Yamamoto et al., 2006) or plastocyanin (Last and Gray, 1990) in chloroplasts failed to improve growth or photosynthesis in transgenic tobacco lines. The existence of several kinetic constraints in photosynthetic electron transport explains why FNR only becomes limiting when it is underexpressed in antisense plants.

It is not evident why overexpression of FNR should give rise to increased tolerance to oxidative stress. Interestingly, homologs of this reductase have been shown to participate in concerted antioxidant responses in many different heterotrophic organisms, including bacteria (Bianchi et al., 1995; Yannone and Burgess, 2001; Krapp et al., 2002; Bittel et al., 2003), yeast (*Saccharomyces cerevisiae*; Li et al., 2001), and protozoa (Girardini et al., 2003), suggesting that it might play a general role in protection against oxidants. We have recently shown that the FNR of *E. coli* provides low potential electrons for repair processes, especially for reductive healing of FeS centers inactivated by superoxide (Giró et al., 2006). This function depends on the NADPH-Fd reductase activity of FNR, which proceeds backward with respect to the physiological photosynthetic direction and is expected to occur only rarely in illuminated leaves. However, this is the most extended function of FNRs in nature, taking place in plant roots and other heterotrophic tissues and organisms (for review, see Ceccarelli et al., 2004). When FNR is expressed in transgenic plants, a considerable fraction of the enzyme accumulates in the stroma (Fig. 2) and, whereas this soluble form cannot engage efficiently in the PETC, it is still able to catalyze electron

transfer from NADPH to low-potential electron acceptors (including Fd) at high rates. It is tempting to speculate that FNR overexpressed in chloroplasts could play a role in repair similar to that undertaken by their counterparts in prokaryotes, but further research is required to rigorously address this possibility.

NADPH-Fd reductase activity of FNR could also contribute to protection by eliminating the excess of reducing equivalents from the PETC. In plants, photooxidative damage stems from the inability of the PETC to handle the surplus of electrons produced by high irradiation or other environmental hardships that inhibit NADPH-consuming reactions of chloroplasts, especially those belonging to the RPPC. These situations often lead to NADPH accumulation, $NADP^+$ shortage, overreduction of the PETC, and adventitious electron and energy transfer to oxygen, resulting in propagation of reactive oxygen species. The introduced FNR may be relieving the reductive burden of the PETC through conversion of NADPH into $NADP^+$ (namely, by regenerating the final acceptor of linear electron flow). We therefore propose that the NADPH-Fd reductase activity of soluble FNR accumulated in the stroma is responsible for the enhanced tolerance of transgenic plants. Research is currently under way to prove this hypothesis. Preliminary observations indicate that introduction into tobacco chloroplasts of a cyanobacterial FNR that is unable to bind to thylakoids (and consequently to productively engage in the PETC), leads to plants with increased stress

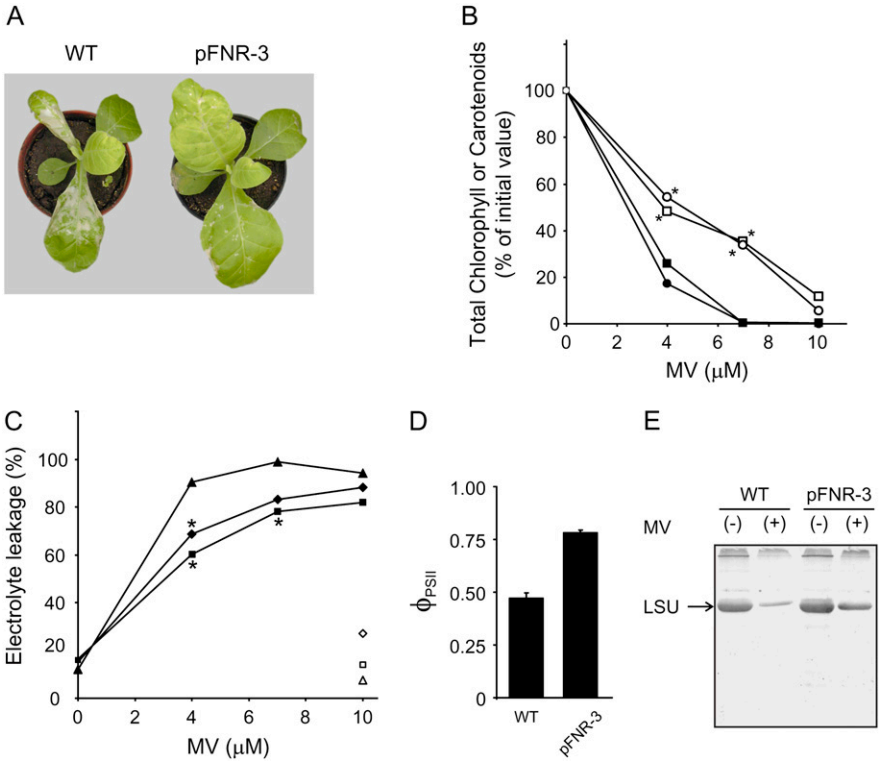

Figure 5. Effect of MV on wild-type and FNR-expressing plants. A, Typical leaf injuries caused by exposure to MV. Four-week old wild-type and transgenic plants were sprayed with 100 μM MV in 0.05% (v/v) Tween 20, and pictures were taken after 3 d of incubation under growth chamber conditions at 150 μmol quanta m^{-2} s^{-1}. The pFNR-3 specimens employed contained 3.5-fold more reductase than wild-type controls. B, MV-induced pigment degradation. Leaf discs from 6-week-old plants were placed on solutions of the indicated concentrations of the herbicide and illuminated at 500 μmol quanta m^{-2} s^{-1} and 25°C during 12 h. Chl (squares) and carotenoids (circles) from wild-type (black symbols) or pFNR-3 (white symbols) plants were determined after MV treatment. Percentages of the initial values are shown. C, MV-induced membrane damage. Ion leakage was estimated by measuring the increase in conductivity of the medium after MV treatment of leaf discs from 6-week-old wild-type (triangles), pFNR-1 (diamonds), and pFNR-3 (squares) plants. White symbols correspond to discs infiltrated with water. In B and C, asterisks indicate significant differences between transgenic and wild-type plants by ANOVA ($P < 0.05$). The pFNR-1 and pFNR-3 specimens employed contained 1.4- and 5.1-fold more reductase than wild-type controls. D, Effect of MV poisoning on the maximal quantum yield (ϕ_{PSII}) of PSII. The ϕ_{PSII} parameter was measured on the fourth fully expanded leaf, 5 h after spraying 4-week-old plants with 100 μM MV and before any visible damage could be detected. E, Oxidative cleavage of Rubisco LSU in plants treated with MV. Extracts were prepared from the fourth fully expanded leaf of 4-week-old plants sprayed with 100 μM MV or mock solution and incubated for 3 d under growth chamber conditions at 150 μmol quanta m^{-2} s^{-1}. Samples corresponding to 2 mg fresh leaf weight were fractionated by SDS-PAGE and blotted onto nitrocellulose membranes for immunodetection with LSU antisera.

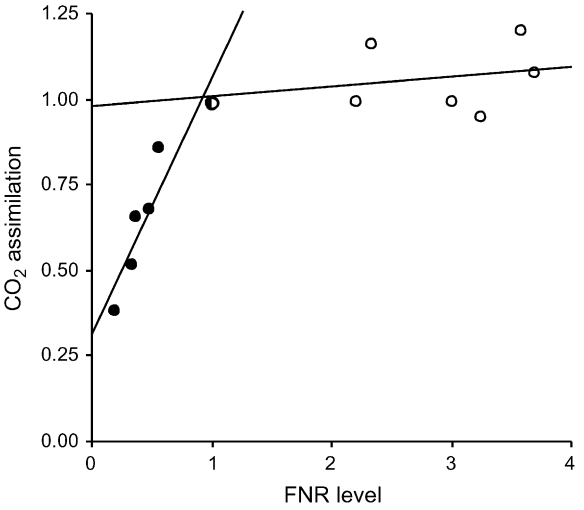

Figure 6. Relationship between CO_2 assimilation and FNR levels. Photosynthesis was measured in FNR antisense (black symbols) and overexpressing (white symbols) transgenic plants at 400 μmol mol^{-1} CO_2 and 2,000 μmol quanta m^{-2} s^{-1}. CO_2 assimilation velocities were normalized with respect to the average wild-type rate (half black/half white symbol), and FNR levels of the various lines were normalized with respect to the average wild-type level. Data of antisense plants are from Hajirezaei et al. (2002).

tolerance without affecting photosynthesis or growth (A. Lodeyro, M. Giró, E.M. Valle, and N. Carrillo, unpublished data).

MATERIALS AND METHODS

Construction of Binary Vectors and Transformation of *Agrobacterium tumefaciens* and Tobacco

A DNA fragment encoding the pea (*Pisum sativum*) FNR precursor was obtained by PCR amplification of a previously isolated gene (Newman and Gray, 1988) with primers 5′-GATGGATCCATCATCAACAACAAC-3′ and 5′-TGCATGATCGTCGACATTATTTCT-3′, containing *Bam*HI and *Sal*I recognition sites, respectively. Amplified DNA was digested with the corresponding enzymes and cloned between the CaMV 35S promoter and polyadenylation regions in pDH51 (Pietrzcak et al., 1986). This construct was excised with *Eco*RI and inserted into the binary vector pCAMBIA2200 (Hajdukiewiez et al., 1994). Recombinant plasmids were verified by DNA sequencing and finally introduced into the genome of tobacco (*Nicotiana tabacum*) cv Petit Havana through Agrobacterium-mediated leaf disc transformation (Gallois and Marinho, 1995). Primary transformants were propagated up to the T_2 generation by self pollination.

Plant Growth and Stress Treatments

Plants were grown on soil in a growth chamber at 80% humidity and a 14-h light/10-h dark photoperiod. Two different light intensities were employed: 150 μmol quanta m^{-2} s^{-1} and 700 μmol quanta m^{-2} s^{-1}, with daytime temperatures of 22°C and 29°C, respectively. The temperature during the dark periods was fixed to 20°C in both cases. Plants were watered twice a week with nutrient medium (Geiger et al., 1999).

To evaluate the effects of excess light, discs (1.2 cm in diameter) were punched from the fourth fully expanded leaf of 6-week-old plants, floated on distilled water with the abaxial side down, and irradiated at 2,000 μmol quanta m^{-2} s^{-1} and 25°C for 17 h, or at 700 μmol quanta m^{-2} s^{-1} and 8°C for the indicated times. Leaf discs treated with MV were placed on solutions containing various concentrations of the herbicide, vacuum infiltrated, and illuminated at 500 μmol quanta m^{-2} s^{-1} and 25°C during 12 h. Electrolyte leakage was measured as the increase in conductivity of the medium, using a Horiba B-173 conductivity meter. To estimate the total ion content of the tissue, discs were autoclaved after the experiment and the conductivity of the resulting solution was determined as above. The results are expressed as the fraction of total electrolytes released after photooxidative treatment.

For treatments of whole plants, 4-week-old specimens were sprayed with 100 μM MV in 0.05% (v/v) Tween 20 and incubated in a growth chamber at 80% humidity and a 14-h light (25°C)/10-h dark (22°C) photoperiod under 150 μmol quanta m^{-2} s^{-1}.

Determination of Photosynthetic Parameters

Net CO_2 uptake rates (A_{CO2}) and intercellular CO_2 concentrations (Ci) were determined according to Hajirezaei et al. (2002), using a portable photosynthesis system LI-6400 (LI-COR). For light response curves, CO_2 concentration of the air entering the leaf chamber and the leaf temperature were adjusted to 400 μmol mol^{-1} and 20°C, respectively, and the light intensity was varied between 20 and 2,000 μmol quanta m^{-2} s^{-1}. For CO_2 response curves, light intensity was adjusted to 400 or 2,000 μmol quanta m^{-2} s^{-1}, and the CO_2 concentration of the air entering the leaf chamber was varied between 50 and 2,000 μmol mol^{-1}. The maximal value of A_{CO2} at light or Ci saturation (A_{max}) and the initial slopes of the corresponding curves were calculated as described in Hajirezaei et al. (2002).

Chl fluorescence was measured using a PAM-2000 portable fluorometer (Walz). F_v and F_m parameters were determined after keeping plants for 60 to 90 min in the dark. Later, plants were exposed first to red light (655 nm, 150 μmol quanta m^{-2} s^{-1}) for 10 min and finally to actinic light (1,000 μmol quanta m^{-2} s^{-1}) for another 10 min. Light-adapted parameters (F'_v and F'_m) were measured at the end of each particular light period. Photosynthetic parameters (F_v/F_m, ϕ_{PSII}, NPQ, and 1 − photochemical quenching parameter [qP]) were calculated as described (Baker and Rosenqvist, 2004).

After photooxidative treatments, the kinetics of relaxation of light-induced NPQ was determined by measuring F_v/F_m every tenth minute during 120 min in wild-type and transgenics plants kept in the dark at 25°C. In all cases, fast kinetics of NPQ relaxation were observed, reaching a steady value of F_v/F_m after 20 min in the dark.

Isolation of Intact Chloroplasts

Chloroplasts were isolated according to Quick et al. (1995). All procedures were carried out at 4°C. Leaves (10 g) were cut into small pieces and homogenized three times (5 s each) in a blender with 100 mL of buffer A containing 50 mM HEPES-KOH, pH 8.0, 330 mM sorbitol, 1 mM $MgCl_2$, 1 mM $MnCl_2$, 2 mM EDTA, 0.1% (w/v) bovine serum albumin, 10 mM ascorbate, and 1 mM glutathione. The homogenate was filtered through three layers of muslin and the filtrate centrifuged for 2 min at 2,000*g*. The supernatant was discarded and the pellet resuspended in 0.5 mL buffer A. Percoll gradients were generated by centrifuging a mixture of 5 mL 2× buffer A plus 5 mL Percoll (Pharmacia) for 50 min at 27,000*g*. The chloroplast suspension was applied on top of the gradient and spun down in a Sorvall HB-4 rotor for 6 min at 9,000*g*. Intact chloroplasts were carefully removed from the higher density band with a Pasteur pipette, diluted in 50 mL buffer A, centrifuged for 2 min at 2,000*g*, and finally resuspended in 1 mL buffer A. Chloroplasts were osmotically shocked in hypotonic buffer containing 50 mM HEPES-KOH, pH 8.0, and 5 mM $MgCl_2$, by incubation in ice for 10 min. After centrifugation at 5,000*g* for 5 min, the resulting supernatant (stroma) was removed and the thylakoid pellet washed with the same buffer, as indicated in the legend to Figure 2. The amount of FNR in these fractions was determined by SDS-PAGE and immunoblotting.

Enzyme Activity Assays

For the identification of enzymes displaying NADPH-dependent diaphorase activity, leaf extracts corresponding to 20 μg of soluble protein were resolved by nondenaturing PAGE on 12% polyacrylamide gels. After electrophoresis, the gel was stained by incubation in 50 mM Tris-HCl, pH 8.5, 0.3 mM $NADP^+$, 3 mM Glc-6-P, 1 unit mL^{-1} Glc-6-P dehydrogenase, and 1 mg mL^{-1} nitroblue tetrazolium until the appearance of the purple formazan bands.

Total FNR activity was also determined in whole broken chloroplasts, stroma, and thylakoids by measuring ferricyanide reduction in a medium containing 50 mM HEPES-KOH, pH 8.0, 5 mM $MgCl_2$, 0.3 mM $NADP^+$, 3 mM

Glc-6-P, 1 unit mL^{-1} Glc-6-P dehydrogenase, 1 mM potassium ferricyanide, and samples corresponding to 0.3 μg chl mL^{-1} (as determined in the total chloroplast fraction). Ferricyanide reduction was monitored by the decrease in absorption at 420 nm, using $\varepsilon_{420} = 1\ mM^{-1}\ cm^{-1}$. One activity unit is defined as the amount of enzyme that catalyzes the reduction of 1 μmol of ferricyanide/min under the conditions described above.

$NADP^+$ photoreduction was measured, using water as electron donor, in 3 mL of 50 mM HEPES-K, pH 8.0, 5 mM $MgCl_2$, 330 mM sorbitol, 0.5 mM $NADP^+$, and thylakoids corresponding to 20 μg chl and 20 μM Fd. Illumination (2,400 μmol quanta $m^{-2}\ s^{-1}$) was provided by a projector lamp and the amount of NADPH formed was estimated by measuring the increase in absorption at 340 nm ($\varepsilon_{340} = 6.2\ mM^{-1}\ cm^{-1}$). $NADP^+$ photoreduction was also determined in the same medium employing 1 mM sodium ascorbate and 33 μM TMPD as the electron donor pair and 2.2 μM DCMU to inhibit electron transport from PSII. MV photoreduction was determined by following oxygen consumption with a Clark-type electrode in a mixture containing 50 mM HEPES-K, pH 8.0, 5 mM $MgCl_2$, 330 mM sorbitol, 0.5 mM sodium azide, 0.1 mM MV, and thylakoids corresponding to 25 μg chl mL^{-1}. All assays were conducted at 25°C.

Analytical Procedures

Extracts were prepared by grinding the fourth fully expanded leaves of control and transgenic plants in liquid nitrogen. The resulting powder was resuspended in 50 mM Tris-HCl, pH 7.5, 5 mM $MgCl_2$, 1 mM EDTA, and 1 mM phenylmethylsulfonyl fluoride. Proteins were determined by the method of Petersen (1977) and resolved by SDS-PAGE on 12% (w/v) polyacrylamide gels as reported previously (Palatnik et al., 1997). Experimental details on western blotting and immunoreaction with specific antisera are also described there. Bands corresponding to FNR in immunoblotted membranes were scanned using the ScanJet 6100C (Hewlett-Packard) and subjected to densitometric analysis with GEL-PRO ANALYZER 3.1 software.

Chls and carotenoids were determined spectrophotometrically after extraction with 80% (v/v) aqueous acetone for leaf homogenates or 96% (v/v) ethanol for leaf discs (Lichtenthaler, 1987).

Received September 28, 2006; accepted December 13, 2006; published December 22, 2006.

LITERATURE CITED

Andersen B, Scheller HV, Møller BL (1992) The PSI-E subunit of photosystem I binds ferredoxin:$NADP^+$ oxidoreductase. FEBS Lett **311:** 169–173

Babbs CF, Pham JA, Coolbaugh RC (1989) Lethal hydroxyl radical production in paraquat-treated plants. Plant Physiol **90:** 1267–1270

Baker NR, Rosenqvist E (2004) Applications of chlorophyll fluorescence can improve crop production strategies: an examination of future possibilities. J Exp Bot **403:** 1607–1621

Batie CJ, Kamin H (1984) Electron transfer by ferredoxin-$NADP^+$ reductase: rapid-reaction evidence for participation of a ternary complex. J Biol Chem **259:** 11976–11985

Bianchi V, Haggard-Ljungquist E, Pontis E, Reichard P (1995) Interruption of the ferredoxin (flavodoxin)-$NADP^+$ oxidoreductase gene of *Escherichia coli* does not affect anaerobic growth but increases sensitivity to paraquat. J Bacteriol **177:** 4528–4531

Bittel C, Tabares LC, Armesto M, Carrillo N, Cortez N (2003) The oxidant-responsive diaphorase of *Rhodobacter capsulatus* is a ferredoxin (flavodoxin)-NADP(H) reductase. FEBS Lett **553:** 408–412

Bouges-Bocquet B (1980) Electron and proton transfer from P-430 to ferredoxin-NADP reductase in *Chlorella* cells. Biochim Biophys Acta **590:** 223–233

Bruns CM, Karplus PA (1995) Refined crystal structure of spinach ferredoxin-$NADP^+$ oxidoreductase at 1.7 Å resolution: oxidized, reduced and 2′-phospho-5′-AMP bound states. J Mol Biol **247:** 1125–1145

Buchanan BB, Schürmann P, Wolosiuk RA, Jacquot JP (2002) The ferredoxin/thioredoxin system: from discovery to molecular structures and beyond. Photosynth Res **73:** 215–222

Carrillo N, Ceccarelli EA (2003) Open questions in ferredoxin-$NADP^+$ reductase catalytic mechanism. Eur J Biochem **270:** 1900–1915

Cassan N, Lagoutte B, Sétif P (2005) Ferredoxin-$NADP^+$ reductase: kinetics of electron transfer, transient intermediates, and catalytic activities studied by flash-absorption spectroscopy with isolated photosystem I and ferredoxin. J Biol Chem **280:** 25960–25972

Ceccarelli EA, Arakaki AK, Cortez N, Carrillo N (2004) Functional plasticity and catalytic efficiency in plant and bacterial ferredoxin-NADP(H) reductases. Biochim Biophys Acta **1698:** 155–165

Desimone M, Henke A, Wagner E (1996) Oxidative stress induces partial degradation of the large subunit of ribulose-1,5-bisphosphate carboxylase/oxygenase in isolated chloroplasts of barley. Plant Physiol **111:** 789–796

Flachmann R (1997) Composition of photosystem II antenna in light-harvesting complex II antisense tobacco plants at varying irradiances. Plant Physiol **113:** 787–794

Forti G, Bracale M (1984) Ferredoxin-ferredoxin-$NADP^+$ reductase interaction: catalytic differences between the soluble and thylakoid-bound complex. FEBS Lett **166:** 81–84

Gallois P, Marinho P (1995) Plant gene transfer and expression protocols. *In* H Jones, ed, Methods in Molecular Biology, Vol 49. Humana Press, Totowa, NJ, pp 39–48

Galtier N, Foyer CH, Huber J, Voelker TA, Huber SC (1993) Effects of elevated sucrose phosphate synthase activity on photosynthesis, assimilate partitioning and growth in tomato (*Lycopersicon esculentum* L. var. UC82B). Plant Physiol **101:** 535–543

Geiger M, Haake V, Ludewig F, Sonnewald U, Stitt M (1999) The nitrate and ammonium supply have a major influence on the response of photosynthesis, carbon metabolism, nitrogen metabolism and growth to elevated carbon dioxide in tobacco. Plant Cell Environ **22:** 1177–1199

Girardini JE, Dissous C, Serra EC (2003) *Schistosoma mansoni* ferredoxin-NADP(H) oxidoreductase and its role in detoxification. Mol Biochem Parasitol **124:** 37–45

Giró M, Carrillo N, Krapp AR (2006) Glucose 6-phosphate dehydrogenase and ferredoxin-NADP(H) reductase contribute to damage repair during the *soxRS* response of *Escherichia coli*. Microbiology **152:** 1119–1128

Haake V, Zrenner R, Sonnewald U, Stitt M (1998) A moderate decrease of plastid aldolase activity inhibits photosynthesis, alters the levels of sugars and starch and inhibits growth of potato plants. Plant J **14:** 147–157

Haehnel W (1984) Photosynthetic electron transport in higher plants. Annu Rev Plant Physiol **35:** 659–693

Haehnel W, Pröpper A, Krause H (1980) Evidence for complexed plastocyanin as the immediate electron donor of P-700. Biochim Biophys Acta **593:** 384–399

Hajdukiewicz P, Svab Z, Maliga P (1994) The small, versatile pPZP family of *Agrobacterium* binary vectors for plant transformation. Plant Mol Biol **25:** 989–994

Hajirezaei MR, Peisker M, Tschiersch H, Palatnik JF, Valle EM, Carrillo N, Sonnewald U (2002) Small changes in the activity of chloroplast $NADP^+$-dependent ferredoxin reductase lead to impaired plant growth and restrict photosynthetic capacity of transgenic tobacco plants. Plant J **29:** 281–293

Harrison EP, Willingham NM, Lloyd JC, Raines CA (1998) Reduced sedoheptulose-1,7-bisphosphatase levels in transgenic tobacco leads to decreased photosynthetic capacity and altered carbohydrate accumulation. Planta **204:** 27–36

Holtgrefe S, Bader KP, Horton P, Scheibe R, von Schaewen A, Backhausen JE (2003) Decreased content of leaf ferredoxin changes electron distribution and limits photosynthesis in transgenic potato plants. Plant Physiol **133:** 1768–1778

Hudson GS, Evans JR, von Caemmerer S, Arvidsson YBC, Andrews TJ (1992) Reduction of ribulose-1,5-bisphosphate carboxylase/oxygenase content by antisense RNA reduces photosynthesis in transgenic tobacco plants. Plant Physiol **98:** 294–302

Kossmann J, Sonnewald U, Willmitzer L (1994) Reduction of the chloroplastic fructose-1,6-bisphosphatase in transgenic potato plants impairs photosynthesis and plant growth. Plant J **6:** 637–650

Krapp AR, Rodriguez RE, Poli HO, Paladini DH, Palatnik JF, Carrillo N (2002) The flavoenzyme ferredoxin (flavodoxin)-NADP(H) reductase modulates NADP(H) homeostasis during the *soxRS* response of *Escherichia coli*. J Bacteriol **184:** 1474–1480

Last DI, Gray JD (1990) Synthesis and accumulation of pea plastocyanin in transgenic tobacco plants. Plant Mol Biol **14:** 229–238

Li J, Saxena S, Pain D, Dancis A (2001) Adrenodoxin reductase homolog

(Arh1p) of yeast mitochondria required for iron homeostasis. J Biol Chem **276:** 1503–1509

Lichtenthaler HK (1987) Chlorophylls and carotenoids: pigments of photosynthetic biomembranes. Methods Enzymol **148:** 350–382

Miyagawa Y, Tamoi M, Shigeoka S (2001) Overexpression of a cyanobacterial fructose-1,6/sedoheptulose-1,7-bisphosphatase in tobacco enhances photosynthesis and growth. Nat Biotechnol **19:** 965–969

Nakatani S, Shin M (1992) The reconstituted $NADP^+$ photoreducing system by rebinding of the large form of ferredoxin-$NADP^+$ reductase to depleted thylakoid membranes. Arch Biochem Biophys **291:** 390–394

Newman BJ, Gray JC (1988) Characterization of a full-length cDNA clone for pea ferredoxin-$NADP^+$ reductase. Plant Mol Biol **10:** 511–520

Palatnik JF, Carrillo N, Valle EM (1999) The role of photosynthetic electron transport in the oxidative degradation of chloroplastic glutamine synthetase. Plant Physiol **121:** 471–478

Palatnik JF, Tognetti VB, Poli HO, Rodriguez RE, Blanco N, Gattuso M, Hajirezaei MR, Sonnewald U, Valle EM, Carrillo N (2003) Transgenic tobacco plants expressing antisense ferredoxin-NADP(H) reductase transcripts display increased susceptibility to photooxidative damage. Plant J **35:** 332–341

Palatnik JF, Valle EM, Carrillo N (1997) Oxidative stress causes ferredoxin-$NADP^+$ reductase solubilization from the thylakoid membranes in methyl viologen-treated plants. Plant Physiol **115:** 1721–1727

Paul MJ, Knight JS, Habash D, Parry MAJ, Lawlor DW, Barnes SA, Loynes A, Gray JC (1995) Reduction in phosphoribulokinase activity by antisense RNA in transgenic tobacco: effect on CO_2 assimilation and growth in low irradiance. Plant J **7:** 535–542

Petersen GL (1977) A simplification of the protein assay method of Lowry et al. which is more generally applicable. Anal Biochem **83:** 346–356

Pierik R, Whitelam GC, Voesenek LACJ, De Kroon H, Visser EJW (2004) Canopy studies on ethylene-insensitive tobacco identify ethylene as a novel element in blue light and plant-plant signalling. Plant J **38:** 310–319

Pietrzcak M, Shillito RM, Hohn T, Potrikus I (1986) Expression in plants of two bacterial antibiotic resistance genes after protoplast transformation with a new plant expression vector. Nucleic Acids Res **14:** 5857–5868

Price GD, Yu JW, von Caemmerer S, Evans JR, Siebke K, Anderson JM, Badger MR (1998) Photosynthesis is strongly reduced by antisense suppression of chloroplastic cytochrome bf complex in transgenic tobacco. Aust J Plant Physiol **25:** 445–452

Quick WP, Scheibe R, Neuhaus HE (1995) Induction of hexose-phosphate translocator activity in spinach chloroplasts. Plant Physiol **109:** 113–121

Soriano GM, Lian-Wang G, de Vitry C, Kallas T, Cramer WA (2002) Electron transfer from the Rieske iron-sulfur protein (ISP) to cytochrome *f in vitro*: is a guided trajectory of the ISP necessary for competent docking? J Biol Chem **277:** 41865–41871

Stark DM, Timmerman KP, Barry GF, Preiss J, Kishore GM (1992) Regulation of the amount of starch in plant tissues by ADP glucose pyrophophorylase. Science **258:** 287–292

Stitt M, Quick WP, Schurr U, Schulze ED, Rodermel SR, Bogorad L (1991) Decreased ribulose-1,5-bisphosphate carboxylase-oxygenase in transgenic tobacco transformed with ''antisense'' *rbcS*. II. Flux control coefficients for photosynthesis in varying light, CO_2, and air humidity. Planta **183:** 555–566

Vallejos RH, Ceccarelli EA, Chan RL (1984) Evidence for the existence of a thylakoid intrinsic protein that binds ferredoxin-$NADP^+$ oxidoreductase. J Biol Chem **259:** 8048–8051

Walker DA, Sivak MN (1986) Photosynthesis and phosphate: a cellular affair? Trends Biochem Sci **11:** 176–179

Witt HT (1971) Energy conversion in the functional membrane of photosynthesis. Analysis by light pulse and electric pulse methods. The central role of the electric field. Biochim Biophys Acta **505:** 355–427

Yamamoto H, Kato H, Shinzaki Y, Horiguchi S, Shikanai T, Hase T, Endo T, Nishioka M, Makino A, Tomizawa K, et al (2006) Ferredoxin limits cyclic electron flow around PSI (CEF-PSI) in higher plants: stimulation of CEF-PSI enhances non-photochemical quenching of Chl fluorescence in transplastomic tobacco. Plant Cell Physiol **47:** 1355–1371

Yannone SM, Burgess BK (2001) The seven-iron FdI from *Azotobacter vinelandii* regulates the expression of NADPH-ferredoxin reductase via an oxidative stress response. J Biol Inorg Chem **3:** 253–258

Yonekura-Sakakibara K, Onda Y, Ashikari T, Tanaka Y, Kusumi T, Hase T (2000) Analysis of reductant supply systems for ferredoxin-dependent sulfite reductase in photosynthetic and nonphotosynthetic organs of maize. Plant Physiol **122:** 887–894

Zhang H, Whitelegge JP, Cramer WA (2001) Ferredoxin-$NADP^+$ oxidoreductase is a subunit of the chloroplast cytochrome b_6f complex. J Biol Chem **276:** 38159–38165